



## ORIGINAL ARTICLE

# Preparation and spectroscopic studies of PbS/nanoMCM-41 nanocomposite



A. Pourahmad \*

Department of Chemistry, Faculty of Science, Rasht Branch, Islamic Azad University, Rasht, Iran

Received 11 April 2011; accepted 22 July 2011

Available online 30 July 2011

## KEYWORDS

Semiconductors;  
PbS nanoparticles;  
Nanocomposites;  
Host–guest chemistry;  
Scanning electron  
microscopy

**Abstract** The present work describes the preparation and characterization of nanosized PbS particles inside the mesopore channels of nanoMCM-41 silicate molecular sieves. The encapsulation of the lead sulfide was carried out at room temperature by ion-exchange method. Diffuse reflectance ultraviolet–visible spectroscopic studies showed a significant shift in the absorption band for the entrapped metal sulfide as compared to corresponding bulk sulfide. Thus, confirming the quantum confinement of the incorporated nanoparticles in nanoMCM-41.

© 2011 Production and hosting by Elsevier B.V. on behalf of King Saud University.

## 1. Introduction

The study of semiconductor nanoparticles has been intensive over the past few years because of their novel optical and electrical properties. These unique properties led to the appearance of many new application areas, such as their use in solar cells, photodetectors, light-emitting diodes, switches and photocatalysts (Pourahmad et al., 2010; Yamamoto et al., 2001). Lead sulfide (PbS) as a unique semiconductor material has been intensively studied in the past decade. PbS nanocrystals are in interest because of the large exciton Bohr radius that gives strong quantum confinement of both electrons and holes, the well developed synthetic protocols, and properties such as multiple carrier generation. PbS is an important binary IV–VI semiconductor mate-

rial with a rather small band gap (0.41 eV at 300 K) (Lee et al., 2002) and a relatively large excitation Bohr radius (18 nm) (Zhao et al., 2005). PbS band gap can be widened to the visible region by forming nanocrystals. Consequently, PbS nanocrystals and nanowires are potentially useful in electroluminescent devices such as light-emitting diodes. Quantum-sized PbS nanoparticles may have applications in light-emitting diodes and high-speed switching, IR detectors (Jing et al., 2008). Moreover, an exceptional third ordered nonlinear optical property of PbS nanoparticles has been found, and it is predicted that as compared with GaAs or CdS with a given particle size, the nonlinear properties of PbS are the best (Warner et al., 2006). The absorption edge of PbS exhibits a large blue shift (Xiang et al., 2004) when one shrinks the crystallite size to the nanometer size regime. Thus, extensive work about its preparation and properties are being implemented. By varying the size and shape from bulk material to nanoparticles, it is possible to change the optical band gap from 0.3 eV to the values up to 5.2 eV. Therefore, it is possible to build optical sensors with adjustable properties. Traditionally, colloidal solutions (Lebedev et al., 2008), porous glasses (Gerber et al., 2009) and certain polymers

\* Tel.: +98 451 2234432; fax: +98 131 4223621.

E-mail address: pourahmad@iaurasht.ac.ir.

Peer review under responsibility of King Saud University.



Production and hosting by Elsevier

(Sadeghi et al., 2009) have been used as hosts for the preparation of nanosized materials. However, they are neither efficient in generating clusters of uniform size nor chemically inert toward the guest molecules. On the other hand, it was realized that the preparation of nanosized materials in zeolitic pores has several advantages and hence they have been considered to form ideal host systems (Sohrabnezhad and Pourahmad, 2007). Indeed, the regular pore structure of zeolite molecular sieves offers a suitable reaction chamber for the controlled assembling of nanostructured materials. However, the smaller pore size of these materials limits their applicability. On the other hand, the recent discovery of mesoporous molecular sieves designated as M41S have broadened the scope of applications. Two of the stable members of the M41S family, viz., hexagonal MCM-41 having unidimensional pore structure and cubic MCM-48 with three-dimensional pore system can comfortably trap the guest molecules in the mesopores. Further, the well-defined pore size, large internal surface area associated with the open framework of the mesophases show promise for such purpose. Therefore, in the present investigation MCM-41 was used as host material, and PbS nanoparticle was selected as the guest molecules.

## 2. Experimental

Nano-sized mesoporous MCM-41 silica with particle size  $\sim 90$  nm was synthesized by a room temperature method with some modification in the described procedure in the literature (Cai et al., 2001). We used tetraethylorthosilicate (TEOS: Merck, 800658) as a source of silicon and hexadecyltrimethylammonium bromide (HDTMABr; BOH, 103912) as a surfactant template for preparation of the mesoporous material. The molar composition of the reactant mixture is as follows:

TEOS : 0.31NaOH : 0.125HDTMABr : 1197H<sub>2</sub>O

The prepared nano-sized MCM-41 was calcined at 550 °C for 5 h to decompose the surfactant and obtain the white powder. The MCM-41 particles prepared from this method are described as nanoMCM-41, in subsequent discussions. Nano-MCM-41 nanoparticles surfactant-free were used for loading the lead sulfide nanoparticles.

As precursors of PbS semiconductors, solution of Pb(CH<sub>3</sub>COO)<sub>2</sub>·2H<sub>2</sub>O (0.1 mol l<sup>-1</sup>) was prepared. To 50 ml of Pb(CH<sub>3</sub>COO)<sub>2</sub>·2H<sub>2</sub>O solution, 1 g of MCM-41 powder was added and stirred for 12 h at 25 °C. The sample was then washed to remove nonexchanged Pb<sup>2+</sup> and air-dried. Finally, sulphurizing of the Pb<sup>2+</sup> ions was carried out with 0.1 M Na<sub>2</sub>S solution. To make the reaction with the S<sup>2-</sup> ion, 1 g Pb<sup>2+</sup>-exchanged mesoporous material was added to 50 ml of 0.1 M solution of Na<sub>2</sub>S at a fixed temperature and magnetically stirred for 2 h. The samples were washed with deionized water and collected by filtration. The obtained samples were fine powders with gray color. The samples were stable at ambient conditions that their color did not change when exposed to the contact of atmospheric moisture. The PbS particles prepared from MCM-41 are described as PbS/nanoMCM-41, in subsequent discussions.

The X-ray diffraction (XRD) pattern was recorded on a Seisert Argon 3003 PTC using nickel-filtered XD-3a CuK $\alpha$  radiations ( $\lambda = 1.5418$  Å). The UV-vis diffused reflectance

spectra (UV-vis DRS) was obtained from UV-vis Scinco 4100 spectrometer with an integrating sphere reflectance accessory. BaSO<sub>4</sub> was used as a reference material UV-vis absorption spectra were recorded using a Shimadzu 1600 pc in the spectral range of 190–900 nm. Scanning electron microscopy (SEM) images of fabricated PbS nanoparticles were obtained using LEO 440i electron microscope. The specific surface area and pore volume of the samples were calculated according to the Brunauer–Emmett–Teller (BET) method. Infrared spectra on KBr pellet were measured on a Bruker spectrophotometer.

## 3. Results and discussion

The surface morphology of nanoMCM-41 nanoparticles and PbS/nanoMCM-41 is investigated by SEM and the micrographs are presented in Fig. 1. Fig. 1(a) shows the SEM image of nanoMCM-41 nanoparticles where small spherical particles of nanomesoporous silica nanoMCM-41 with diameters of  $\sim 90$  nm are evident. There is no considerable change in morphology of PbS/nanoMCM-41.

Fig. 2 shows the XRD patterns of nanoMCM-41 template and PbS loading on the template. Measurements of the samples were carried out in the  $2\theta$  different ranges ( $2\theta = 2$ – $10^\circ$  and  $2\theta = 10$ – $80^\circ$ ), under the conditions of 40 kV and 40 mA,

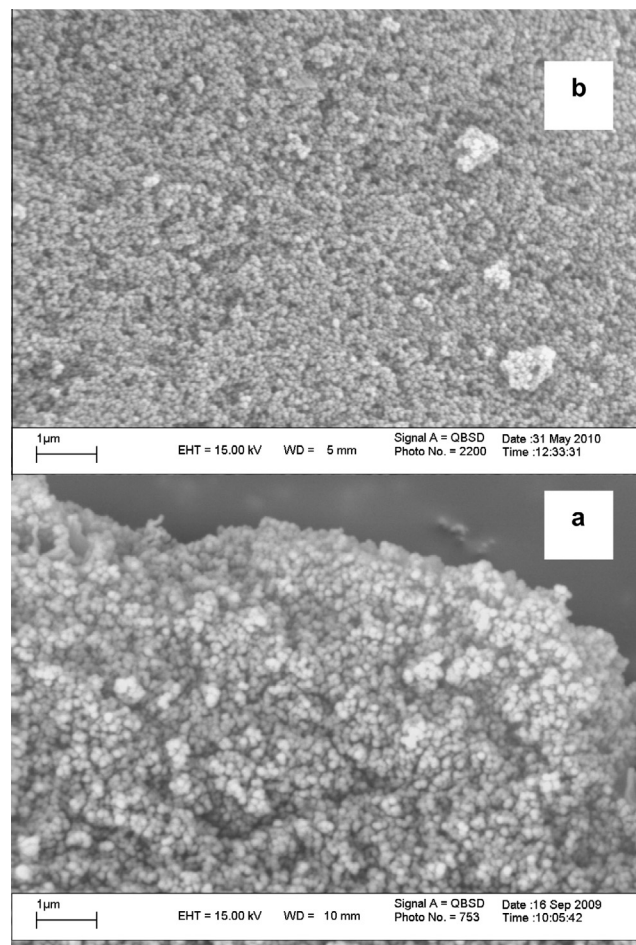


**Figure 1** Scanning electron microscopy (SEM) micrographs of (a) nanoMCM-41 and (b) PbS/nanoMCM-41.

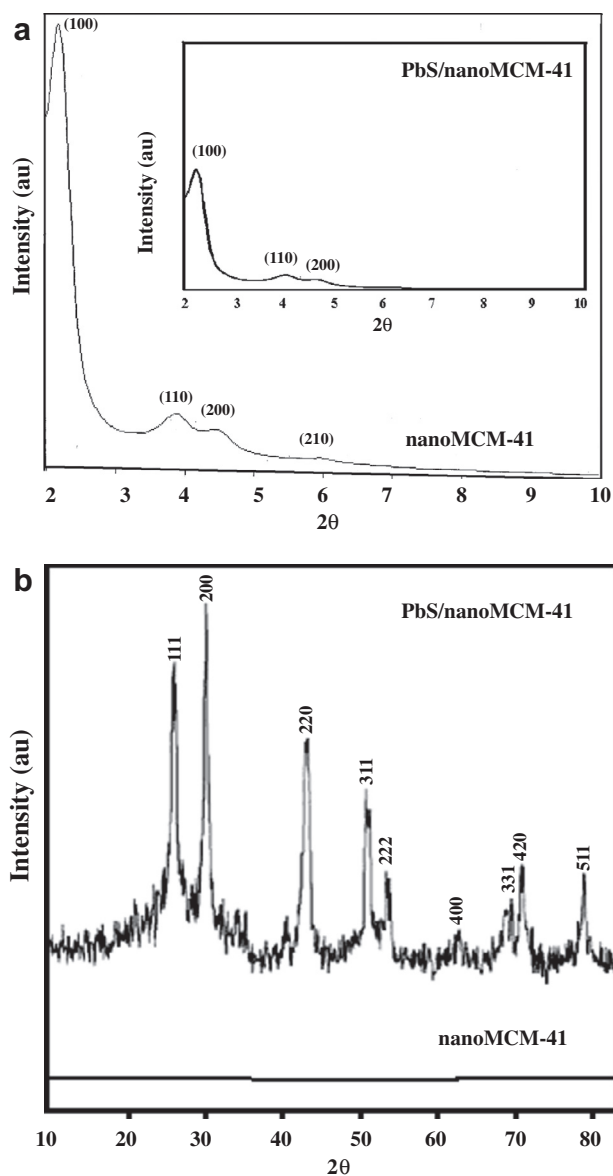


**Figure 2** (a) X-ray diffraction patterns of nanoMCM-41 and PbS/nanoMCM-41 in range  $2\theta = 2\text{--}10^\circ$  and (b) X-ray diffraction patterns of nanoMCM-41 and PbS/nanoMCM-41 in range  $2\theta = 10\text{--}80^\circ$ .

at a step size of  $2\theta = 0.02^\circ$ . Fig. 2(a) shows low angle X-ray diffraction patterns of calcined nanoMCM-41 nanoparticles and PbS/nanoMCM-41. The pattern of the product clearly exhibits four well-defined peaks which can be indexed with (1 0 0), (1 1 0), (2 0 0), and (2 1 0) planes on hexagonal unit cell, indicating mesoporous structure of nanoMCM-41. The peak appearing at low angle ( $2\theta = 2.2$ ) corresponds to (1 0 0) the plane of nanoMCM-41 indicating ordered pore structure of nanoMCM-41, which can be attributed to quasi-two dimensional hexagonal lattice of nanoMCM-41 (Beck et al., 1992). In this figure, we observed that both X-ray patterns are very similar. But, some differences, such as the broadening and slight shifting to higher angles of the diffraction peaks as well as the decrease of their intensity can be observed in the spectra. This should be attributed to the

porefilling effects that can reduce the scattering contrast between the pores and the framework nanoMCM-41 materials. These decreases of the peak intensities are in agreement with the reported results for other zeolites (Sathish et al., 2006; Sadjadi et al., 2007). High angle X-ray diffraction pattern ( $2\theta = 10\text{--}80$ ), Fig. 2(b), further supports the presence of PbS. All reflection peaks of the product can be indexed as a pure face-centered cubic structure. The broadened diffraction peaks in Fig. 2(b) indicated that the particle sizes of the product were very small. We have determined the nanoparticles size by using the Debye–Scherrer formula,  $d = 0.9\lambda / \beta \cos \theta$ , where  $d$  is the average diameter of the crystalline,  $\lambda$  the wavelength of X-ray,  $\beta$  the excess line width of the diffraction peak in radians and  $\theta$  the Bragg angle. Based on this analysis the average size of PbS nanoparticles has been found to be 3 nm (Table 1).

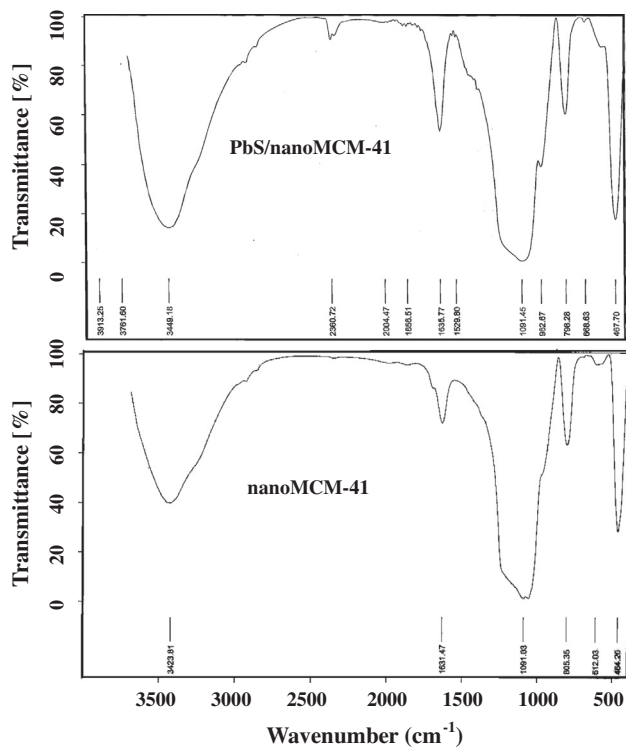
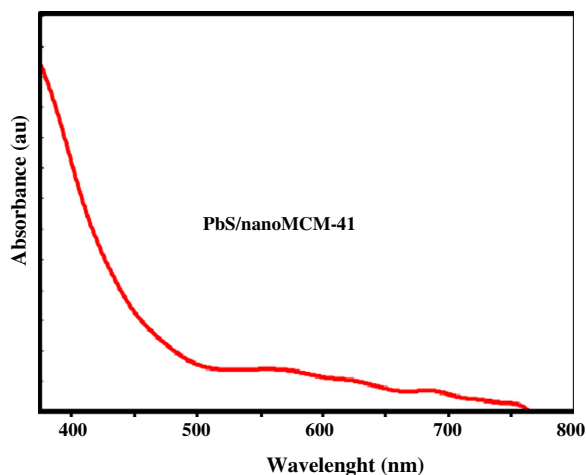
The results of the specific surface area and pore volume measurements (BET measurements) for nanoMCM-41 and PbS/nanoMCM-41 show that the pore volumes of the host mesoporous material, which was  $1.05 \text{ ml g}^{-1}$  for nanoMCM-41, decreased to  $0.80 \text{ ml g}^{-1}$  for PbS/nanoMCM-41 materials. Similarly, the specific surface areas of the composite materials were decreased from  $850 \text{ m}^2 \text{ g}^{-1}$  for nanoMCM-41 to  $700 \text{ m}^2 \text{ g}^{-1}$  for PbS/nanoMCM-41. Decreasing of the volumes of the pores and the specific surface area of the mesoporous material demonstrates that the guests are located in the channels (Table 1).

The IR spectra of nanoMCM-41 and PbS/nanoMCM-41 samples in the range of  $400\text{--}4000 \text{ cm}^{-1}$  are shown in Fig. 3. The broad absorption band in the region of  $3765\text{--}3055 \text{ cm}^{-1}$  can be attributed to the stretching of the framework Si–OH group with the defective sites and physically adsorbed water molecules. The vibrations of Si–O–Si can be seen at  $1091 \text{ cm}^{-1}$  (asymmetric stretching),  $805 \text{ cm}^{-1}$  (symmetric stretching) and  $454 \text{ cm}^{-1}$  (bending) (Sohn et al., 1986; Umamaheswari et al., 2002). In the present work, all bands in PbS/nanoMCM-41 sample show a shift to higher wave numbers with respect to the nanoMCM-41 mesoporous material. This shift reveals that nanoparticles could incorporate in nanoMCM-41 mesoporous material. The increased intensity is observed in nanoparticles sample with respect to nanoMCM-41. This increase related to the extent of perturbation of T–O–T vibrations of the mesoporous material lattice (bands  $400\text{--}1700 \text{ cm}^{-1}$ ) and increase acidic bridged hydroxyls vibrations ( $3423 \text{ cm}^{-1}$  band) (Sun and Sachtler, 2003). These kinds of differences related to present PbS nanoparticles in nanoMCM-41.

The UV–vis diffused reflectance spectrum (UV–vis DRS) for PbS nanoparticles prepared from nanoMCM-41 matrices is shown in Fig. 4. The bulk PbS gave an absorption at 3020 nm (Wise, 2000). Comparing the absorption edge of bulk PbS to that of PbS/nanoMCM-41 sample prepared from mesoporous materials, it is seen that a large blue shift in the onset of absorption is observed in this sample. This blue shift indicates that PbS exists as small clusters within the mesoporous material pores as reported by several researchers (Smotkin et al., 1988; Chen et al., 1997). This was supported by a significant decrease in the surface area of PbS/nanoMCM-41, compared to the parent mesoporous material (Table 1). This phenomenon of a blue shift of absorption edge has been ascribed to a decrease in particle size. It is well known that in the case of semiconductors the band gap between the valence and conduction band increases as the size of the particle decreases in the nanosize range.

**Table 1** Band gap, specific surface area, particle size, pore volume and absorption edge of samples.

	Band gap (eV)	Specific surface area (m <sup>2</sup> g <sup>-1</sup> )	Particle size (nm)	Pore volume (cc/g)	Absorption edge (nm)
nanoMCM-41	—	850	90	1.05	—
PbS/nanoMCM-41	2.05	700	3	0.80	514

**Figure 3** IR spectra of nanoMCM-41 and PbS/nanoMCM-41.**Figure 4** UV-vis absorption spectrum of PbS/nanoMCM-41.

This results in a shift in the absorption edge to a lower wavelength region. The magnitude of the shift depends on the particle size of the semiconductor. In the present study, the PbS/nanoMCM-41 samples prepared from the

nanoMCM-41 matrix showed a blue shift of approximately 2500 nm compared to the bulk particles. From the onset of the absorption edge, the band gap of the PbS particles was calculated using the method of Tandon and Gupta (1970) (Table 1). The size of PbS nanoparticles, estimated based on the results of Weller et al. (Vossmeier et al., 1994) was 3 nm for PbS/nanoMCM-41 sample.

#### 4. Conclusions

In this paper, we have reported a simple method to synthesize PbS nanoparticles in nanoMCM-41 material hosts. A large blue shift in the absorption edge was observed in the samples prepared by an ion-exchange method, indicating the formation of nanometer-sized PbS nanoparticles in nanoMCM-41 mesopore, as a consequence of particle size effects.

#### Acknowledgements

We thank the Research Vice Presidency of Islamic Azad University, Rasht Branch for their encouragement, permission and financial support.

#### References

- Beck, J.S., Vartuli, C., Roth, W.J., Leonowicz, M.E., Kresge, C.T., Schmitt, K.D., Chu, C.T-W., et al., 1992. A new family of mesoporous molecular sieves prepared with liquid crystal templates. *J. Am. Chem. Soc.* 114, 10834–10843.
- Cai, Q., Luo, Zh.-Sh., Pang, W.Q., Fan, Yu-W., Chen, Xi-H., Cui, Fu-Zh., 2001. Dilute solution routes to various controllable morphologies of MCM-41 silica with a basic medium. *Chem. Mater.* 13, 258–263.
- Chen, W., Wang, Z., Lin, L., 1997. Thermoluminescence of CdS clusters in zeolite-Y. *J. Luminescence.* 71, 151–156.
- Gerber, R.W., Leonard, D.N., Franzen, S., 2009. Conductive thin film multilayers of gold on glass formed by self-assembly of multiple size gold nanoparticles. *Thin Solid Films* 517 (24), 6803–6808.
- Jing, S., Xing, S., Wang, Y., Hu, H., Zhao, B., Zhao, C., 2008. Synthesis of 3D well-packed octahedral PbS nanocrystal arrays. *Mater. Lett.* 62, 977–979.
- Lebedev, V.S., Vitukhnovsky, A.G., Yoshida, A., Kometani, N., Yonezawa, Y., 2008. Absorption properties of the composite silver/dye nanoparticles in colloidal solutions. *Colloids Surf. A* 326 (3), 204–209.
- Lee, S.M., Jun, Y.W., Cho, S.N., Cheon, J.W., 2002. Single-crystalline star-shaped nanocrystals and their evolution: programming the geometry of nano-building blocks. *J. Am. Chem. Soc.* 124, 11244–11245.
- Pourahmad, A., Sohrabnezhad, Sh., Radaee, E., 2010. Degradation of Basic Blue 9 dye by CoS/nanoAlMCM-41 catalyst under visible light irradiation. *J. Porous Mater.* 17 (3), 367–375.
- Sadeghi, B., Sadjadi, M.A.S., Vahdati, R.A.R., 2009. Nanoplates controlled synthesis and catalytic activities of silver nanocrystals. *Superlattices Microstruct.* 46 (6), 858–863.

- Sadjadi, M.S., Pourahmad, A., Sohrabnezhad, Sh., Zare, K., 2007. Formation of NiS and CoS semiconductor nanoparticle inside mordenite-type zeolite. *Mater. Lett.* 61, 2923–2926.
- Sathish, M., Viswanathan, B., Viswanathan, R.P., 2006. Alternate synthetic strategy for the preparation of CdS nanoparticles and its exploitation for water splitting. *Int. J. Hydrogen* 31, 891–898.
- Smotkin, E.S., Lee, Chongmok., Bard, A.J., Campion, A., Fox, M.A., Mallouk, et al., 1988. Size quantization effects in cadmium sulfide layers formed by a Langmuir–Blodgett technique. *Chem. Phys. Lett.* 152, 265–268.
- Sohn, J.R., DeCanio, S.J., Lunsford, J.H., Odonnell, D.J., 1986. Determination of framework aluminium content in dealuminated Y-type zeolites: a comparison based on unit cell size and wavenumber of i.r. bands. *Zeolites* 6, 225–227.
- Sohrabnezhad, Sh., Pourahmad, A., 2007. New methylene blue (NMB) encapsulated in mesoporous AlMCM-41 material and its application for amperometric determination of ascorbic acid in real samples. *Electroanalysis* 15, 1635–1641.
- Sun, A., Sachtler, W.M.H., 2003. Mn/MFI catalyzed reduction of  $\text{NO}_x$  with alkanes. *Appl. Catal. B* 42, 393–401.
- Tandon, S.P., Gupta, J.P., 1970. Measurement of forbidden energy gap of semiconductors by diffuse reflectance technique. *Phys. Status Solidi* 38, 363–367.
- Umamaheswari, V., Palanichamy, M., Murugesan, V., 2002. Isopropylation of m-Cresol over mesoporous Al-MCM-41 molecular sieves. *J. Catal.* 210, 367–374.
- Vossmeier, T., Katsikas, L., Giersig, M., Popovic, I.G., Diesner, K., Chemseddine, A., Eychmuller, A., Weller, H., 1994. CdS nanoclusters—synthesis, characterization, size dependent oscillator strength, temperature shift of the excitonic transition energy, and reversible absorbance shift. *J. Phys. Chem.* 98, 7665–7673.
- Warner, J.H., Heckenberg, N., Rubinsztein-Dunlop, H., 2006. Non-linear photoluminescence from purified aqueous PbS nanocrystals. *Mater. Lett.* 60, 3332–3334.
- Wise, F.W., 2000. Lead salt quantum dots: the limit of strong quantum confinement. *Acc. Chem. Res.* 33, 773–780.
- Xiang, J., Yu, S-H., Liu, B., Xu, Y., Gen, X., Ren, L., 2004. Shape controlled synthesis of PbS nanocrystals by a solvothermal–microemulsion approach. *Inorg. Chem. Commun.* 7, 572–575.
- Yamamoto, T., Kishimoto, S., Lida, S., 2001. Control of valence states for ZnS by triple codoping method. *Phys. B* 308, 916–919.
- Zhao, Y.B., Zou, J.H., Shi, W.F., 2005. In situ synthesis and characterization of lead sulfide nanocrystallites in the modified hyperbranched polyester by gamma-ray irradiation. *J. Mater. Sci. Eng. B* 121, 20–24.